Iran J Sci Technol Trans Civ Eng (2019) 43:273–286
https://doi.org/10.1007/s40996-018-0139-7

REVIEW PAPER

Study of Direct Finite Element Method of Analysing Soil–Structure Interaction in a Simply Supported Railway Bridge Subjected to Resonance

Anand M. Gharad[1] · R. S. Sonparote[1]

Received: 26 April 2016 / Accepted: 23 July 2018 / Published online: 30 July 2018

Abstract
This paper presents the dynamic soil–bridge interaction under high-speed railway lines, under different soil stiffness conditions. Starting from the analysis of a simply supported Euler–Bernoulli beam model subjected to moving loads, a three-dimensional multi-body (soil–abutment–bridge–ballast–sleeper–rail) model formulated in the time domain to study the vibrations induced due to the passage of moving concentrated loads was analysed using the direct finite element method of soil–structure interaction analysis. The high-speed train was considered to be a set of concentrated loads, the rail was modelled as a Euler–Bernoulli beam (frame element), and the sleepers, ballast, bridge, abutments and soil were modelled using eight-node solid (brick) elements. Layered soil stratum's effects on the dynamic response of the bridge deck and variation of stresses were studied. From this study, it was observed that the direct method of FE analysis can be an effective tool to solve the complex dynamic soil–structure interaction problems.

Keywords Dynamic soil–bridge interaction · Moving loads · 3D continuum model · Newmark-β integration · Layered soil

1 Introduction

The dynamic behaviour of high-speed railway bridges is one of the most studied problems in civil engineering. The phenomenon of resonance takes place when the operating speed of high-speed railway becomes close to the fundamental frequency of bridge. This leads to vibrations and the problems related to the safety, train stability and passengers comfort. Hence, the dynamic behaviour of high-speed railways cannot be ignored. Immense literature about the dynamic response of railway bridges is available. Yang and Yau (1997), Yang et al. (1997, 1999) and Yau et al. (1999) studied the impact response of bridges to high-speed trains and the interaction of vehicle–bridge systems (VBI). In this, complex VBI elements are developed to simulate the interaction behaviour between the bridge and the high-speed railway systems moving over it. Frýba (2001) developed a theoretical model of a bridge using the integral transformation method, which provided an estimate of the amplitude of free vibrations.

To study the vibration response of railway bridges, the engineering community has used various moving models, namely the force model, the mass model and the oscillator model (Museros and Alarcón 2005; Museros and Martínez-Rodrigo 2007; Martínez-Rodrigo and Museros 2011; Pesterev et al. 2003; Liu et al. 2009). The numerical approaches, such as finite element method (FEM), for modelling complex structures have gained importance in the last few years. Delgado and Cruz (1997) studied the dynamic behaviour of railway bridges assuming the moving mass model and the train model traversing on a bridge model made up of finite elements. Wu et al. (2001) developed a sophisticated 3D vehicle–rail–bridge interaction (VRBI) model to study the dynamic interaction between the moving trains and a railway bridge, considering the effects due to track irregularities. A substantial increase in the response

✉ Anand M. Gharad
anandgharad@gmail.com

R. S. Sonparote
rssonparote@apm.vnit.ac.in

[1] Department of Applied Mechanics, Visvesvaraya National Institute of Technology, Nagpur, India

of both train and bridge due to the track irregularities is found. Song et al. (2003) developed a new three-dimensional bridge deck model consisting of variable-node nonconforming flat shell (NFS) elements, to study the high-speed train–bridge interaction. These elements have high performance in dynamic problems, especially for discontinuities due to complicated track structures. Ju and Lin (2003) performed a simply supported multi-span bridge pier resonant analysis using a three-dimensional FEM system. The fundamental train frequency and the first bridge natural frequency in each direction were recommended to be as different as possible to prevent resonance. Cheng et al. (2001) developed a new bridge–vehicle–track element to examine the moving train–railway track–bridge interaction. The moving vehicles were modelled as a two-degree-of-freedom mass–spring–damper system, which is added to an upper beam that simulates the rails and a lower beam to model the bridge deck. Biondi et al. (2005) compared the work of Cheng et al. (2001) with the sub-structure technique.

A great deal of experimental work to study the dynamic response of the existing multi-span bridges under high-speed lines was reported by Xia et al. (2003, 2005, 2006). The purpose of these experimental works was to collect the dynamic response data and compare the data with the sophisticated vehicle (train)–bridge numerical model(s).

Most civil engineering structures are supported by soils/rocks. As the supporting soil is much larger in size than the structure itself, it is considered infinite in dimension (unbounded). This system of structure and soil can be subjected to static or dynamic loads. To determine the actual response of the structure under dynamic actions, dynamic soil–structure interaction analysis has to be performed. This complex phenomenon can be solved using two methods, namely the sub-structure method and direct method (Wolf 1985, 1986). The sub-structure method divides the soil–structure system into two parts, namely the super-structure that may include a portion of soil in the vicinity of the structure and the remaining, an unbounded soil domain. The direct method considers a definite extent of half-space soil–structure model in a continuous manner, with the only distinction being in material property. The sub-structure and direct method work in frequency and time domains, respectively. In the direct method, to achieve accurate dynamic response of the structure connected with the soil, it is essential that the waves propagate and decay in all the directions and travel to far fields. Lysmer and Waas (1972) and Kausel et al. (1975) and Kausel and Roesset (1977) developed wave-transmitting boundaries, and Song and Wolf (1996) considered the extended mesh concept to account for the proper boundary condition at finite domains.

A rigorous dynamic soil–structure–high-speed moving vehicle interaction analysis has gained attention in recent years. Hanazato et al. (1991) and Pyl et al. (2004a, b) studied the effect of dynamic soil–road under traffic on the adjacent buildings and structures. Ülker-Kaustell et al. (2010) in their work presented a qualitative analysis of the dynamic SSI of a portal frame railway bridge based on the linear theory of elasticity. Using simple concepts from the finite element theory, the influence of SSI on the dynamic properties of the structure and its response due to the high-speed load model (HSLM) of the Eurocode1 was found out.

Recently, Romero et al. (2013) have investigated the soil–structure interaction's (SSI's) influence on a small simply supported railway bridge response. A three-dimensional FE and boundary element (BE) numerical model was developed to study the dynamic SSI of a bridge, in the time domain. It is noticed that the resonant train speeds reduce due to soil–bridge interaction, whereas the fundamental periods and damping ratios of the response increase due to SSI. Many complex parameters such as the spring–dashpot model to represent the articulated train, track irregularities and most importantly the BE-FE formulations were used to solve this 3D dynamic soil–bridge interaction problem. For the systems with complicated geometry and material properties, application of BEM has proven to be difficult. BEM cannot be applied directly for the analysis of soil–structure system. It is to be used with FEM.

The structural designers' community is always in search of a simple approach to achieve rapid and appropriate solutions for such complex problems, with the use of commercial software packages. Thus, it is necessary to develop a simplified approach for the analysis of a full-scale 3D soil–bridge model, which can be easily implemented and analysed in relevant commercial software. To do this, a direct finite element method to analyse dynamic soil–bridge interaction is attempted using commercial software package capable of analysing moving loads problems (SAP2000 2014). Study related to 3D continuum soil–bridge interaction analysis subjected to high-speed moving loads cannot be seen. In this work, a full-scale 3D continuum dynamic soil–bridge interaction analysis under simple moving loads, to verify the resonance response of a simply supported bridge is presented. Since the resonance response of the bridge alone is considered, the track irregularities are neglected (Yang et al. 2004).

This paper presents the verification of dynamic analysis for the passage of high-speed trains on Euler–Bernoulli beam, in SAP2000 finite element (FE) program. Further, the development of a three-dimensional finite element numerical model to study the dynamic soil–structure interaction in time domain (Fig. 1) is presented. The direct method of analysing soil–structure interaction is used to

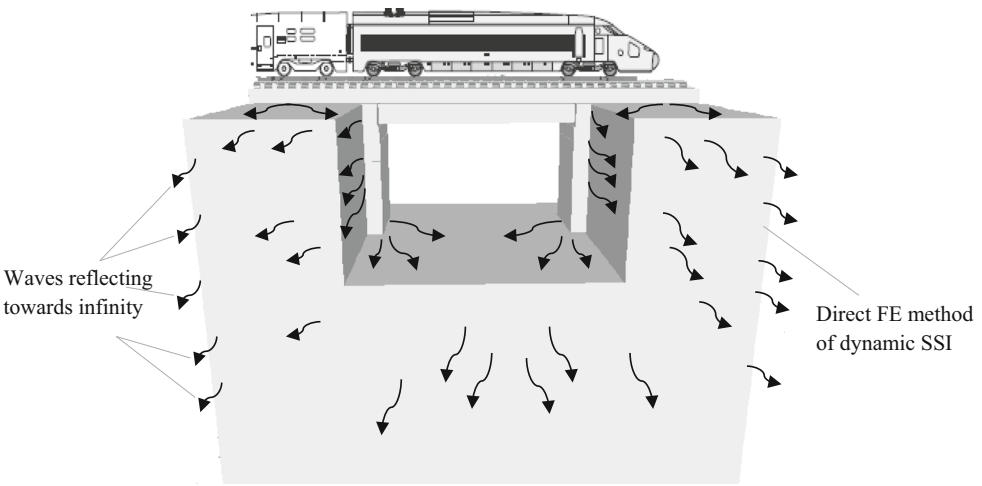

Fig. 1 Moving loads–track–soil–structure interaction

study this numerical model. Changes in modal parameters are studied considering different types of soils. The effect of these soils on the resonance response of the deck slab is then studied. Dynamic soil–bridge interaction analysis under moving loads, for layered soil, has not yet been performed. Thus, a case study on the 3D continuum soil model, to study the dynamic response of the deck slab, is carried out by considering the layered soil.

2 Analytical Solution for Moving Forces

The closed form solution for vertical displacement $y(x, t)$ and acceleration $a(x, t)$ response of a simply supported Euler–Bernoulli beam (Fig. 2) of span L subjected to row of N axel forces F_n, where n= 1, 2, 3,…, N, moving with constant speed 'v' along the beam, at a distance x with respect to time t is represented by Eqs. (1) and (2), respectively (Frýba 2001).

$$y(x,t) = \sum_{j=1}^{\infty}\sum_{n=1}^{N} y_0 \frac{F_n}{F} j\omega\omega_1^2 [f(t-t_n)h(t-t_n) - (-1)^j f(t-T_n)h(t-T_n)] \sin\left(\frac{j\pi x}{L}\right), \quad (1)$$

where

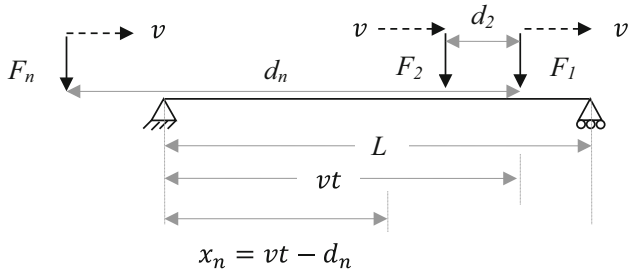

Fig. 2 Movement of series of forces over a simply supported beam

$$f(t) = \frac{1}{\omega_j' D}\left[\frac{\omega_j'}{j\omega}\sin(j\omega t+) - e^{-\omega_D t}\sin\left(\omega_j' t + \varphi\right)\right] \quad (1.1)$$

$$\omega = \frac{\pi v}{L} \quad (1.2)$$

$$\omega_j'^2 = \omega_j^2 - \omega_D^2 - 2i\omega_D\omega_j \quad (1.3)$$

$$D^2 = \left[\left(\omega_j'^2 + \omega_D^2\right) - j^2\omega^2\right] + 4j^2\omega^2\omega_D^2 \quad (1.4)$$

$$\lambda = \arctan\left[\frac{-2j\omega\omega_D}{\left(\omega_j'^2 + \omega_D^2\right) - j^2\omega^2}\right] \quad (1.5)$$

$$\varphi = \arctan\left[\frac{2\omega_D\omega_j'}{\omega_D^2 - \omega_j'^2 + j^2\omega^2}\right]. \quad (1.6)$$

$$a(x,t) = \sum_{j=1}^{\infty}\sum_{n=1}^{N} y_0 \frac{F_n}{F} j\omega\omega_1^2 [\ddot{f}(t-t_n)h(t-t_n) - (-1)^j \ddot{f}(t-T_n)h(t-T_n)] \sin\left(\frac{j\pi x}{L}\right), \quad (2)$$

where

$$\ddot{f}(t) = -\frac{\omega_j'^2 - \omega_D^2}{\omega_j' D}\left[\frac{j\omega\omega_j'}{\omega_j'^2 - \omega_D^2}\sin(j\omega t + \lambda) - e^{-\omega_D t}\sin\left(\omega_j' t + \varphi'\right)\right] \quad (2.1)$$

$$\varphi' = \varphi + \arctan\left[\frac{2\omega_D\omega_j'}{\omega_j'^2 - \omega_D^2}\right], \quad (2.2)$$

where y_0 is the displacement at the centre of the beam, F_n is the nth axle force, ω. is the circular frequency, ω_D is the circular frequency of the damping, ω_1 is the first circular frequency, t is the time, and t_n and T_n are time instants when the nth force F_n enters and leaves the beam. j is the

natural vibration mode of a damped beam with $j = 1, 2, 3,\ldots$; $h(t)$ stands for the Heaviside unit function related to time t as:

$$h(t) = \begin{cases} 0 & \text{or } t < 0 \\ 1 & \text{for } t \geq 0. \end{cases} \quad (3)$$

The solution for displacements and accelerations can be obtained by using the mutual relations of the Fourier integral transform and its derivation can be confirmed, in Ref. (Frýba 2001). The analytical solutions help in understanding the basic principles of the dynamic system, investigating the key parameters, and their significance.

2.1 Numerical Modelling

For a multi-degree-of-freedom lumped mass system, the force equilibrium conditions can be expressed as a function of time, as a sum of forces with different origins, as follows (Chopra 2008):

$$\mathbf{m_j\ddot{u}_j} + \mathbf{f_{Dj}} + \mathbf{f_{Sj}} = \mathbf{p_j(t)}, \quad (4)$$

where $\mathbf{m_j}$ is the mass at j levels $(j = 1, 2, \ldots, n)$, $\mathbf{f_{Dj}}$ is the damping force, $\mathbf{f_{Sj}}$ is the elastic (or inelastic) resisting force, and $\mathbf{p_j(t)}$ is the external force. In finite element method, Eq. (4) can be solved using direct integration technique. Finite element (FE) techniques perform discretization in spatial coordinates for linear and nonlinear behaviours of any structure. This discrete multi-degree-of-freedom system of equations can be expressed as:

$$\mathbf{m\ddot{u}} + \mathbf{c\dot{u}} + \mathbf{ku} = \mathbf{p(t)}, \quad (5)$$

where e, **c** and **k** are the mass, damping and stiffness matrices, respectively, **(t)** the load vector (from moving loads), and **u**, **u̇** and **ü** the vectors of nodal displacement, velocity and acceleration. Equation (5) was solved using Newmark-β method (Chopra 2008).

The simplest procedure to represent the load train (moving loads) in FE method is to apply load pulse time histories for each node, depending on the time of arrival and the discretization (Fig. 3).

The damping matrix c was considered proportional to the mass matrix m and the stiffness matrix k as:

$$c = a_0 m + a_1 k. \quad (6)$$

The damping ratio for the nth mode of such a system is

$$\zeta_n = \frac{a_0}{2}\frac{1}{\omega_n} + \frac{a_1}{2}\omega_n. \quad (7)$$

The coefficients a_0 and a_1 can be determined from specified damping ratios ζ_i and ζ_j for the ith and jth modes, respectively. If both the modes are assumed to have the same damping ratio ζ, which is reasonable based on experimental data, then

$$a_0 = \zeta\frac{2\omega_i\omega_j}{\omega_i + \omega_j}; a_1 = \zeta\frac{2}{\omega_i + \omega_j}. \quad (8)$$

The damping is then found out from Eq. (6), and the damping ratio for any other mode, given by Eq. (7), varies with natural frequency as shown in Fig. 4.

2.2 Validation of Dynamic Response

The analytical solution of a simply supported bridge of span 40 m with a damping ratio of 1%, bending stiffness of 280.1329 × 10^6 kN/m^2 and line mass of 30 ton/m subjected to HSLM-A3 (Eurocode1 2008) moving along the span can be seen in Henriques (2007). An attempt was made to analyse the same problem using SAP2000 FE program. In this FE analysis, frame elements of 1 m length each were considered to model the bridge. The support conditions were hinged. The displacement and acceleration responses as shown in Fig. 5 at the bridge mid-span for the train load travelling at resonant speed were validated with the analytical solution.

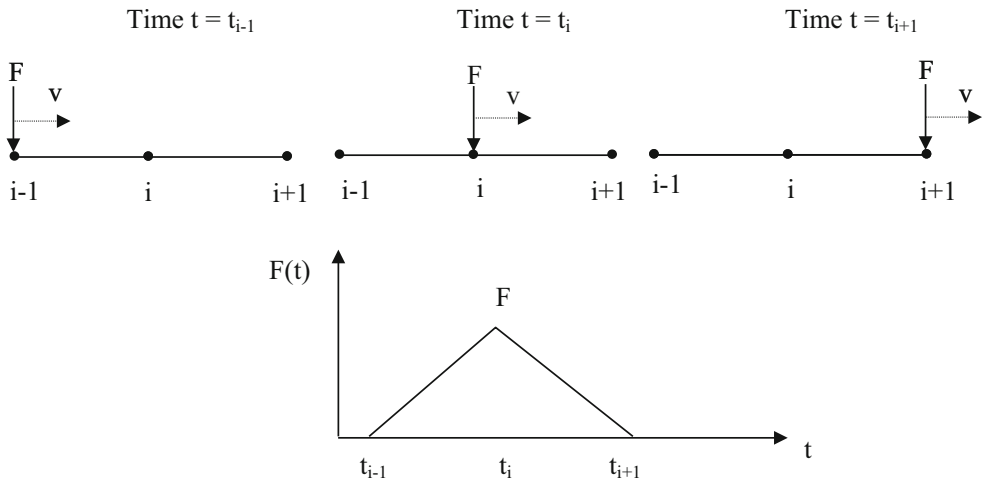

Fig. 3 Load function variation on node i in finite element model

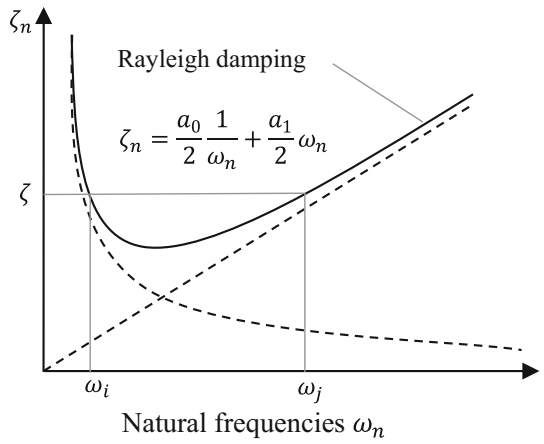

Fig. 4 Rayleigh damping

From Fig. 6, it can be seen that the displacement and acceleration responses have a fair agreement with the analytical solution. For moving trains travelling on the beam, the resonant condition of the beam can be derived as follows (Teng et al. 2008):

$$v_{\mathrm{brn},i} = \frac{3.6 f_{\mathrm{bn}} \cdot d}{i} (n = 1, 2, 3\ldots; i = 1, 2, 3\ldots), \quad (9)$$

where $v_{\mathrm{brn},i}$ is the resonant moving train's velocity (km/h); f_{bn} is the nth natural frequency of the beam (Hz); d is the characteristic distance of the moving high-speed trains (HST) (m); and i represents the number of complete oscillation cycles for the nth mode of the beam to vibrate during the passage of two adjacent loads (Wang et al. 2010). For the aforesaid problem, the natural frequency corresponding to first mode was found to be 18.786 rad/s and the characteristic distance was taken as load interval which was approximately 20 m. From this, the resonant velocity $v_{\mathrm{br1},1}$ was evaluated as 215.28 km/h. From Fig. 5, it is evident that the resonant velocity calculated is in fair agreement with the FEM solution. Finally, it can be stated that the agreement between both approaches is verified and, therefore, the method followed for performing the dynamic analyses in SAP2000 FE program for the passage of high-speed trains can be used. In the following sections, direct method of analysing soil–structure interaction, using SAP2000 FE program, is presented.

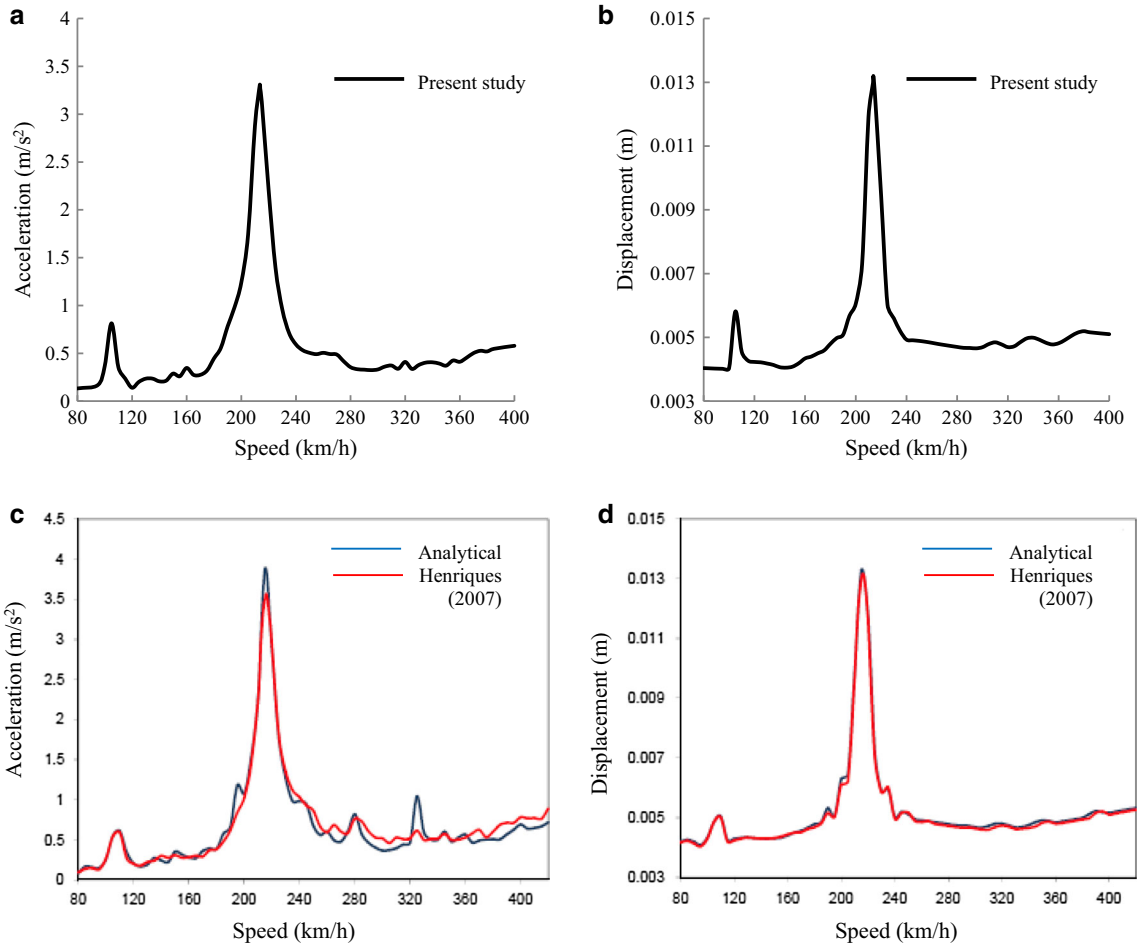

Fig. 5 Mid-span vertical acceleration (**a**) and displacement (**b**) responses, present study. Mid-span vertical acceleration (**c**) and displacement (**d**) responses with blue solid line obtained by analytical solution and red solid line given by Henriques (2007)

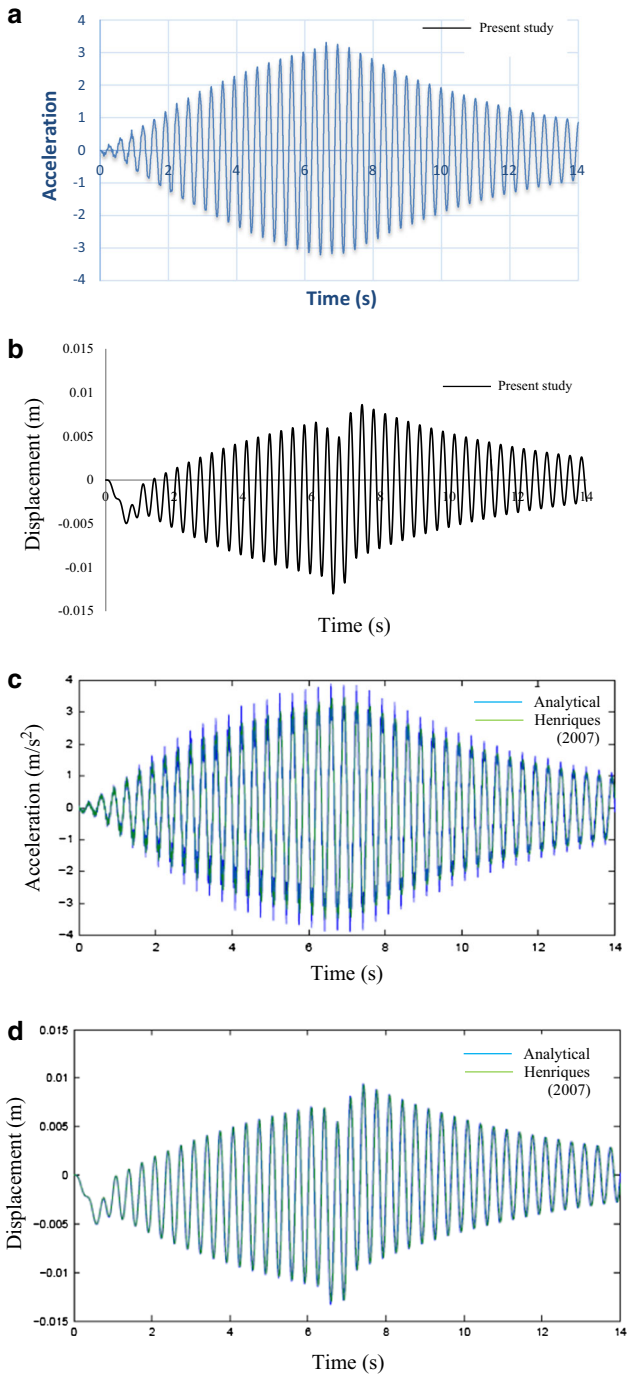

Fig. 6 Mid-span vertical acceleration (**a**) and displacement (**b**) plots at resonant speed, present study. The figure also shows the mid-span vertical acceleration (**c**) and displacement (**d**) plots at resonant speed with blue solid line obtained by analytical solution and green solid line given by Henriques (2007).

3 3D Soil–Structure Interaction Model

The underlying soil medium significantly affects the dynamic response of a structure. In addition, due to wave radiation to infinity, damping is developed by a homogeneous soil stratum (von Estorff 1991). In this paper, a three-dimensional direct finite element method for analysis of soil–structure interaction is used to explore the dynamic soil–structure behaviour.

In the direct method, modelling of linear regular soil adjacent to the soil–structure interface leads to many degrees of freedom. It can be advantageous from a computational point of view to introduce generalized coordinates, especially when the total dynamic system behaves linearly and when (frequency-independent) springs, dashpots and masses are used to model the transmitting boundary (Wolf 1988). It was assumed that there is no separation between sleepers and ballast and between soil and the adjoining structures; hence, a perfect bond is assumed. Viscous dampers were assumed to simulate the silent boundaries. These silent boundaries were represented with damping coefficients c_n and c_t at each node in the normal and tangential directions (Wolf 1988):

$$c_n = A\rho c_p; c_t = A\rho c_s, \tag{10}$$

where c_p represents the dilatational wave velocity, c_s represents the shear wave velocity, A represents the applicable area, and ρ represents the density of soil. The velocity of a dilatational and shear waves is controlled by the shear modulus (G) as (Wolf 1988):

$$c_p = \sqrt{\frac{(\lambda + 2G)}{\rho}}; c_s = \sqrt{\frac{G}{\rho}}, \tag{11}$$

where

$$\lambda = \frac{E}{(1+v)(1-2v)} \quad \text{and} \quad G = \frac{E}{2(1+v)}. \tag{11.1}$$

E and v are the modulus of elasticity and Poisson's ratio, respectively.

Figure 7 shows the three-dimensional continuum soil–structure model with viscous dampers simulating the silent boundaries.

3.1 High-Speed Train (HST) Model

The train type considered in this paper was referred from Romero et al. (2013). The authors considered one front traction car, eight passenger cars and one rear traction car. Passenger cars adjacent to traction cars shared one bogie with the neighbouring passenger car, while central passenger cars shared both bogies with the neighbouring cars. Bogie distances and axle distances of the articulated HST were 3 and 18.7 m, respectively (Fig. 8). The mass of different parts of the HST is summarized in Table 1.

Moving loads model (Fig. 9) was considered (Doménech and Museros 2011). This model does not take into account the inertial effects of the train masses, and

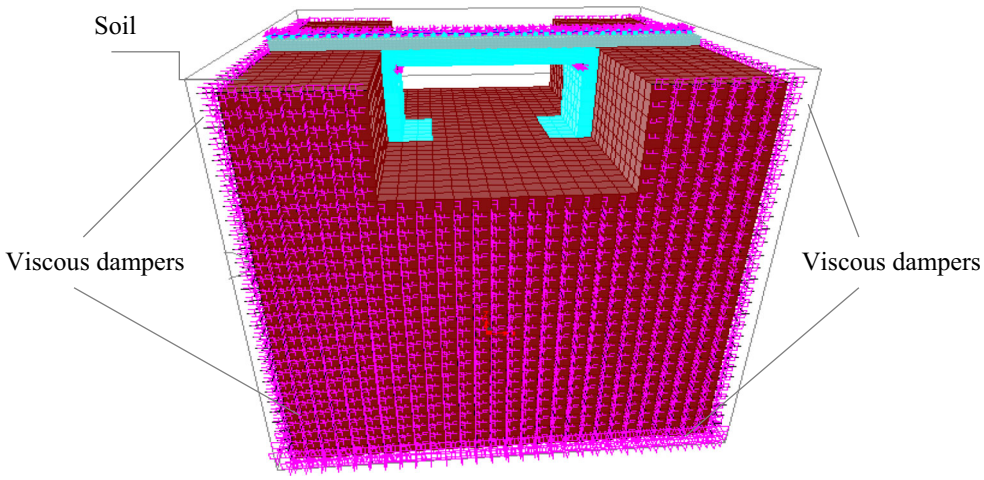

Fig. 7 Three-dimensional continuum soil–structure model with viscous dampers

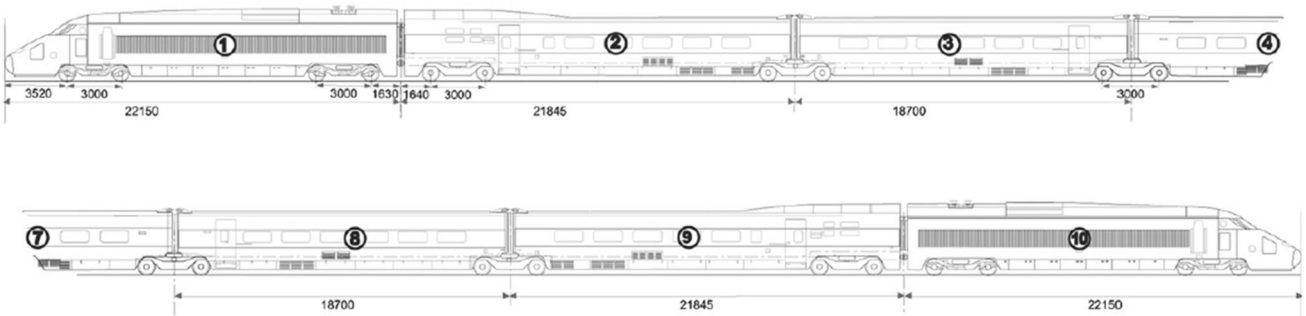

Fig. 8 Schematic representation of HST configuration

Table 1 Summary of the mass of various parts of HST

Description	Name	Traction cars	Passenger cars	Unit
Mass of car body	M_c	55,790	24,000	kg
Mass of bogie	M_b	2380	3040	kg
Mass of wheel axle	M_w	2048	2003	kg

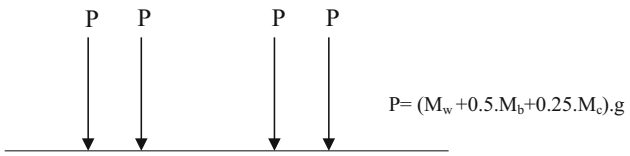

Fig. 9 Moving loads vehicle model

therefore, the train is modelled as a series of concentrated, constant-valued loads travelling at constant speed. Nevertheless, the multi-body model of HST as studied by the authors in Ref. (Romero et al. 2013) furnishes a sophisticated analysis approach; the closed form solutions of the equations of motion for the moving loads model can easily be obtained.

3.2 High-Speed Railway Bridges

In this section, the dynamic soil–bridge interaction analysis is presented. A simply supported 12-m-long railway bridge considered by Romero et al. (2013) was studied. The deck (Fig. 10a) was composed of a 0.2-m-thick concrete slab. The slab rested over five pre-stressed concrete beams with a 0.8 × 0.3 m rectangular cross section. The width of the slab was 6 m. The concrete properties were the following: density $\rho = 2500$ kg/m^3, Poisson's ratio $v = 0.2$ and Young's modulus $E = 31 \times 10^9$ N/m^2. The deck leaned over two concrete abutments (Fig. 10b) with the following properties: density $\rho = 2500$ kg/m^3, Poisson's ratio $v = 0.3$ and Young's modulus $E = 20 \times 10^9$ N/m^2. The beams rested on laminated rubber bearings. The thickness of the bearings was 20 mm, and their stiffness and damping values were 560×10^6 N/m and 50.4×10^3 Ns/m, respectively. A single ballast track was located over the deck. The track was composed of two rails with a bending stiffness of EI = 6.45×10^6 Nm^2 and a mass per unit length of 60.3 kg/m for each rail. The rail pads had a thickness of 10 mm and stiffness and damping values of 150×10^6 N/m and 13.5×10^3 Ns/m, respectively. The pre-stressed concrete mono-block sleepers had the

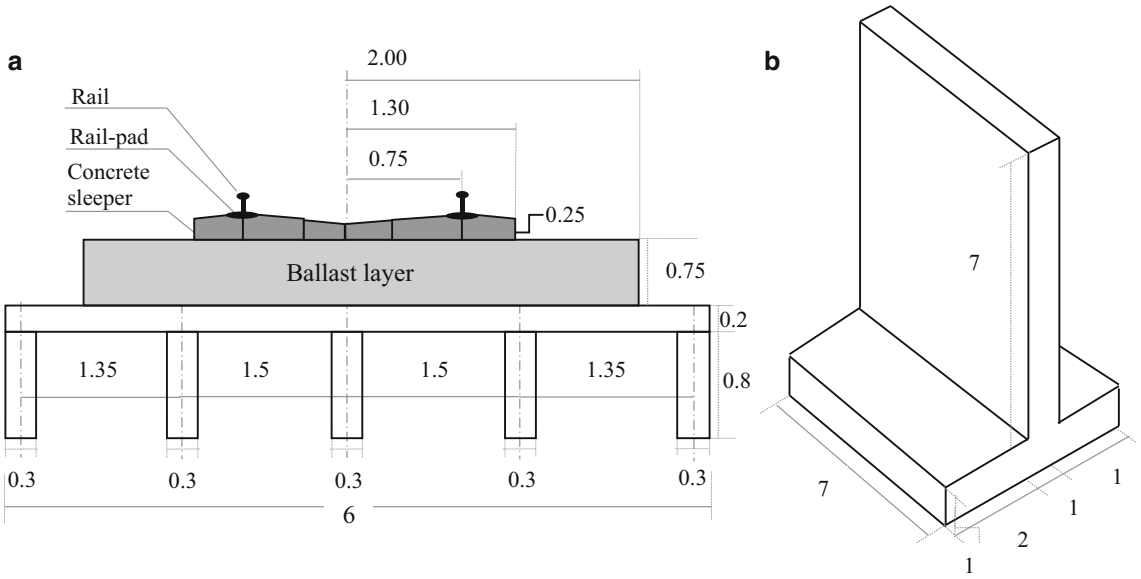

Fig. 10 **a** Cross section of bridge deck. **b** Abutment dimensions. All dimensions are in metres

following characteristics: length $l = 2.60$ m, width $w = 0.25$ m, height 0.25 m (under the rail) and mass 300 kg. A distance $d = 0.6$ m between the sleepers was considered. The ballast had a density of ρ =1800 kg/m^3, Poisson's ratio of $\nu = 0.2$ and Young's modulus of $E = 209 \times 10^6$ N/m^2. The width of the ballast was 4.00 m, and the height was $h = 0.75$ m. The structure was assumed to be located on top of the soil. The soil was a homogeneous viscoelastic soil with Poisson's ratio $v = 0.35$ and mass density ρ =1800 kg/m^3. Table 2 summarizes the aforesaid information. The rails were modelled as Bernoulli–Euler beam elements, and the sleepers, ballast, abutments and soil were modelled as eight-node brick element, whereas the rail–pads were modelled as spring–damper elements. Four different S-wave velocities were analysed, corresponding to a soil with infinite stiffness ($C_s = \propto$ m/s), a hard soil (C_s = 400 m/s), a medium soil (C_s = 250 m/s) and a soft soil (C_s = 150 m/s). Soil–bridge discretization is shown in Fig. 7.

Table 2 Summary of properties of soil–bridge parameters

Description	Properties	Value	Unit
Concrete slab and pre-stressed beams	Mass density ρ	2500	kg/m^3
	Poisson's ratio v	0.2	–
	Young's modulus E	31×10^9	N/m^2
Concrete abutments	Mass density ρ	2500	kg/m^3
	Poisson's ratio v	0.3	–
	Young's modulus E	20×10^9	N/m^2
Bearings	Stiffness	560×10^6	N/m
	Damping	50.4×10^3	Ns/m
Rails	Bending stiffness EI	6.45×10^6	Nm^2
	Mass per unit length	60.3	kg/m
Rail pads	Stiffness	150×10^6	N/m
	Damping	13.5×10^3	Ns/m
Concrete sleepers	Mass	300	kg
Ballast	Mass density ρ	1800	kg/m^3
	Poisson's ratio v	0.2	–
	Young's modulus E	209×10^6	N/m^2
Soil	Poisson's ratio v	0.35	–
	Mass density ρ	1800	kg/m^3

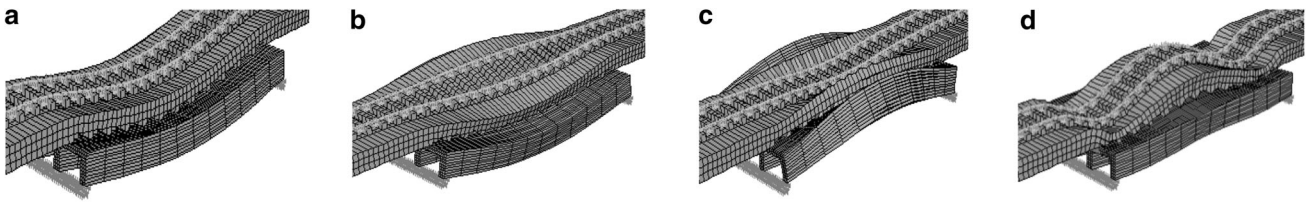

Fig. 11 Four natural frequencies: **a** f_1=11.90 Hz. **b** f_2 = 14.57 Hz. **c** f_3 = 26.16 Hz. **d** f_4 = 41.5 Hz, and mode shapes of the structure

3.3 Dynamic Soil–Structure Interaction

When the frequency of an external force matches the fundamental frequency of the structure, resonance occurs. Also, a lightly damped structure initiates a resonant regime. Four natural frequencies and the mode shapes of the simply supported rail–bridge structure are shown in Fig. 11. These natural frequencies are comprised of the following modes: (1) symmetric bending mode, (2) torsional mode, (3) symmetric bending of cross-sectional mode and (4) antisymmetric bending mode shape. The response of a structure in terms of deflections, moments, etc., is of special importance in structural engineering. Many researchers have considered the higher modes' contributions to compute these important parameters. But, for the maximum acceleration response of simply supported railway bridges, the contribution of the first symmetric and antisymmetric bending modes is essential (Museros and Alarcón 2005). Hence, in the present study, these two modes are considered.

As discussed earlier, the damping matrix is obtained by assigning the same damping ratio of 2% (assumed for reinforced concrete, Eurocode1 2008) to these modes considering $\omega_i = \omega_1$ and $\omega_j = \omega_4$. Rayleigh damping parameter values from Eq. 7 are a_0 2.32 s^{-1} and $a_1 = 1.192 \times 10^{-4}$ s. The damping of the system was evaluated by using free vibration analyses. Table 3 summarizes the results of fundamental frequencies and damping ratios for the different soil types considered.

Table 3 Results of dynamic soil–bridge interaction for various modal properties and resonant speeds

Soil type	c_s (m/s)	f_1 (Hz)	ζ_1	$v_{1,2}$ (m/s)
Infinitely stiff	–	11.90	0.020	111
Hard soil	400	10.90	0.029	101
Medium soil	250	9.96	0.042	95
Soft soil	150	7.84	0.056	73.4

It is evident from Table 3 that for different soil types, the soil–structure interaction leads to a decrease in frequency and an increase in damping ratio for various soil types.

3.4 Soil–Structure Vibrations

Resonance of a bridge excited by a row of moving forces is expressed by Eq. (9). Figure 12 shows the maximum vertical acceleration at the centre of the deck for a range of train speeds between 30 and 130 m/s (108 km/h and 468 km/h, respectively). The deck acceleration was found to increase with train speed. Considering the characteristic distance between bogies of d = 18.7 m, maximum accelerations were reached at resonant speeds corresponding to the first bending mode shape. Figure 12 also shows maximum vibration levels at speed $v_{1,2}$ = 111 m/s when soil–bridge interaction was not considered. The response of the structure changed significantly when soil–structure interaction was considered. The second resonant speed of the

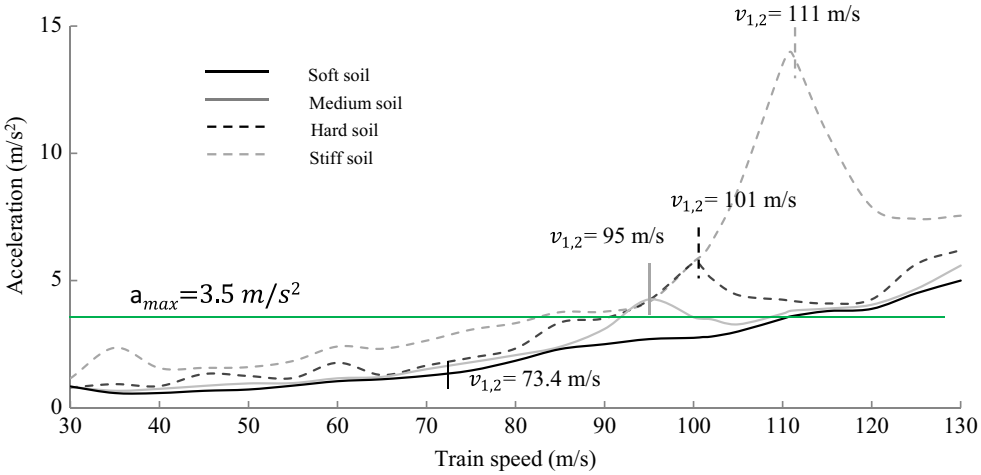

Fig. 12 Maximum vertical acceleration at the centre of the mid-span deck for $C_s = \infty$ m/s (grey dashed line), C_s = 400 m/s (black dashed line), C_s = 250 m/s (grey solid line) and C_s = 150 m/s (black solid line) for different train speeds. The second resonant speeds of the first mode are marked with vertical lines

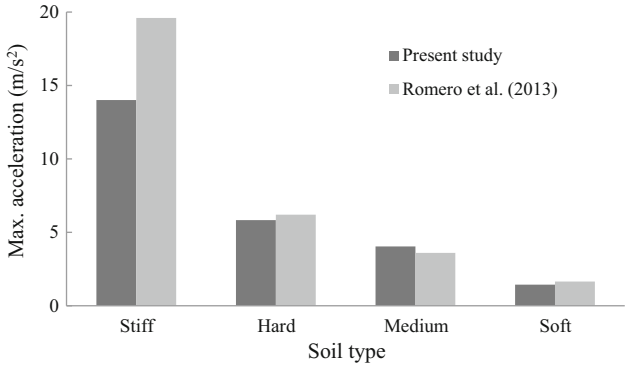

Fig. 13 Comparison chart of maximum mid-span bridge deck vertical acceleration values at resonant speeds for different types of soils

first mode shape decreased to $v_{1,2} = 101$ m/s and $v_{1,2} = 95$ m/s for hard and medium soils, respectively, due to the change in the dynamic behaviour of the system (Table 3). No resonant effects occurred with soft soil. Nevertheless, the resonant speed for soft soil was $v_{1,2} = 73.4$ m/s. In all soil types (except for infinitely stiff soil), the maximum acceleration at the centre of the mid-span deck was below $a_{max} = 3.5$ m/s^2, this is the limit set by the European Committee for Standardization (CEN) (Eurocode1 2008).

The results presented here are compared with the results discussed by Romero et al. (2013). The nature of curves and maximum vertical accelerations for three soils (hard, medium and soft) have a fair agreement with those presented by authors, but for the infinitely stiff soil case, a significant reduction in the maximum acceleration value for the corresponding resonant speed is observed (Fig. 13). Since in this study the effect of dynamic SSI on bridge deck vibrations is emphasized, their results are closely examined. A small variation between the results of the present study and the referred article is observed (Fig. 13) due to the slight change in the dimensions of the deck cross section and abutment geometry.

Figure 12 shows the vertical acceleration time histories at the centre of the mid-span deck for speed $v_{1,2}$ and the acceleration limit for a ballasted track of $a_{max} = 3.5$ m/s^2 (Eurocode1 2008). Figure 14a–c represents a variation in the response of the structure with consecutive passage of loads. The vertical acceleration response with each passage of travelling loads was more when SSI was excluded. It was interesting to note that the vertical acceleration response was reduced for lower soil stiffness, and the magnification of response was almost absent in soft soil (Fig. 14d).

4 Case Study

A case study was worked out to examine the effect of layered soil and the HST model (same as discussed in above section) on the dynamic response of the mid-span

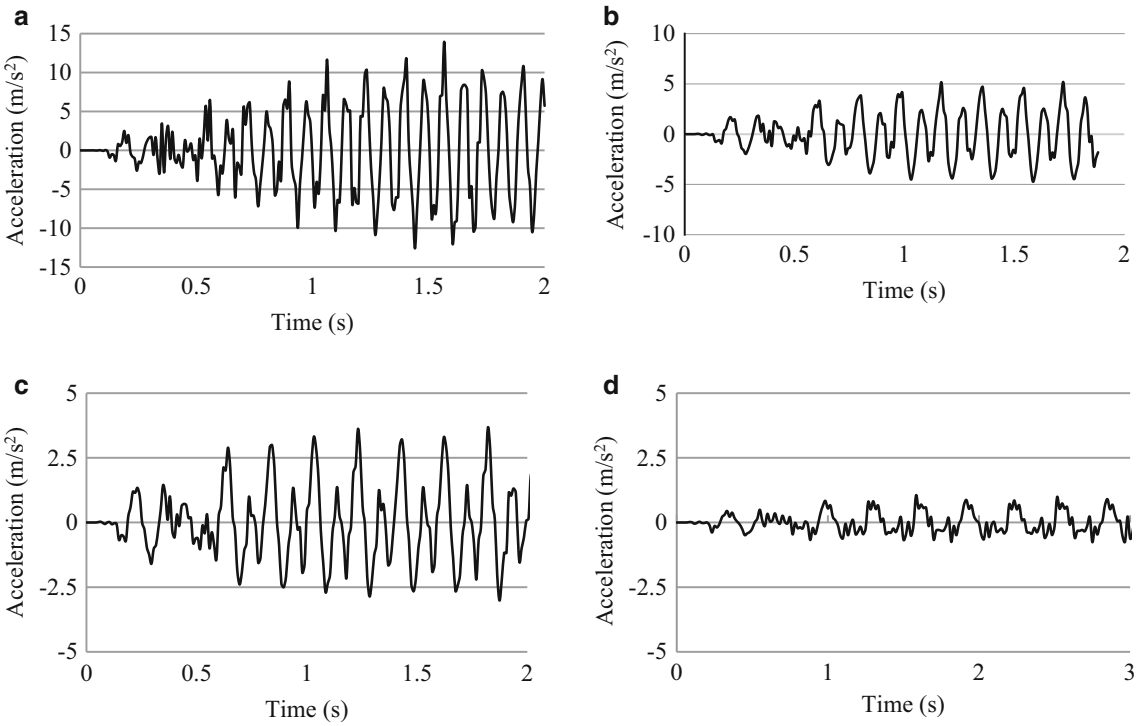

Fig. 14 Vertical acceleration time histories at the centre of the mid-span deck for an HST of moving loads travelling at **a** $v = 111$ m/s, **b** $v = 101$ m/s, **c** $v = 95$ m/s and **d** $v = 73.4$ m/s on **a** infinitely stiff soil, **b** hard soil, **c** medium soil and **d** soft soil

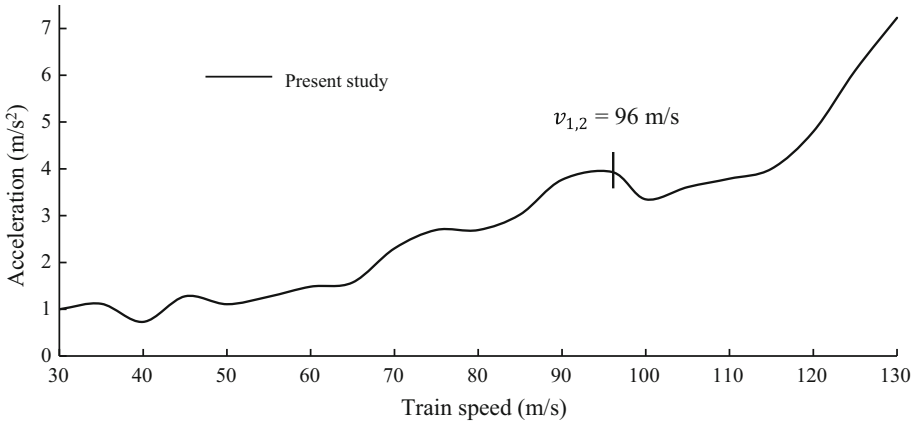

Fig. 15 Maximum vertical acceleration at the centre of the mid-span deck at different train speeds for a layered soil

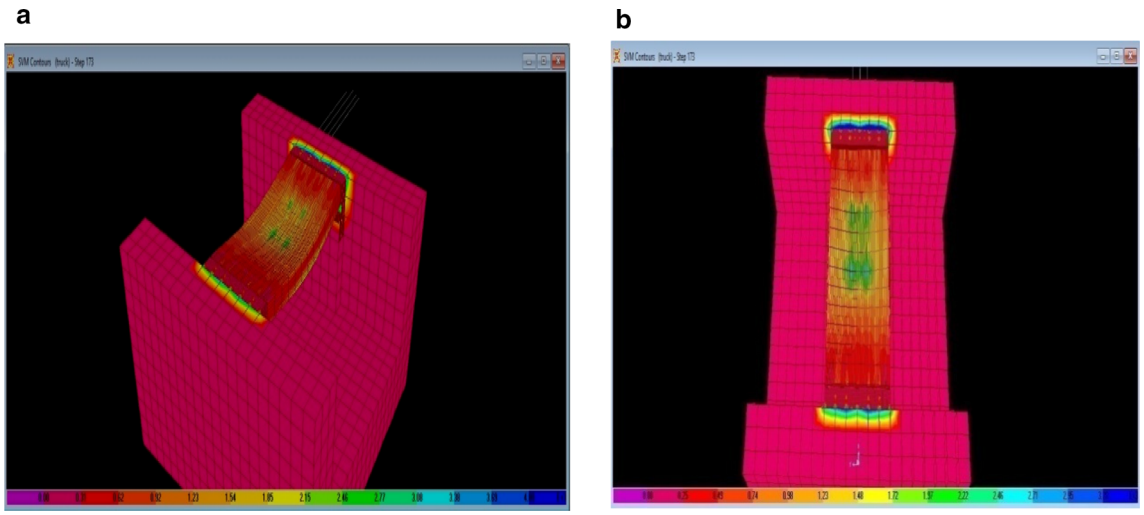

Fig. 16 von Mises stress contours: **a** 3D view and **b** plan of continuum model for the resonant train speed v = 96 m/s of layered soil

section of the deck slab. The properties of elastic half-spaced layered soil were referred from Rajasankar et al. (2007). Following properties were assumed. Hard rock stratum up to a height of 12 m from bottom with shear wave velocity of 1390 m/s and bulk unit weight of 28 kN/m^3; weathered rock stratum up to a height of 6 m above hard rock with shear wave velocity of 571 m/s and bulk unit weight of 26 kN/m^3; compressible clay stratum up to a height of 10 m above weathered rock with shear wave velocity of 307 m/s and bulk unit weight of 17 kN/m^3; and dense sand layer up to a height of 2 m above compressible clay with shear wave velocity of 235 m/s and bulk unit weight of 18.5 kN/m^3.

The second resonant speed of the first mode shape (f_1 = 10.372 Hz) and the system damping from free vibration analyses of layered soil were $v_{1,2}$ = 96 m/s and 0.0363, respectively. Figure 15 shows the maximum vertical acceleration at the centre of the deck corresponding to a range of train speeds between 30 and 130 m/s (108 and 468 km/h, respectively), for the layered soil system.

4.1 Stress Analysis Between Abutment and Soil

Stress variation during the analysis was studied to identify the critical values at the interface between the abutment and layered soil. A discontinuity of thickness or modulus leads to the discontinuity in stress (Cook et al. 2004). Thus, effective/von Mises stresses were considered to observe the interface stress variation. Figure 16 representing the stress contours manifests the maximum stresses at the abutment and soil interface. As the concrete abutment and the adjacent flexible soil may behave independently of the maximum vertical acceleration of the structure, a separation between them may be observed. Further, it was decided to study the effect of stresses developed due to maximum positive vertical acceleration of structure at the interface of abutment and the homogeneous soils. From Fig. 17 it is apparent that maximum stress (dark blue colour) for all the cases is obtained between the rigid abutment and the comparatively flexible soil interface. Hence, a check on the magnitude of stresses developed at the interface will signal

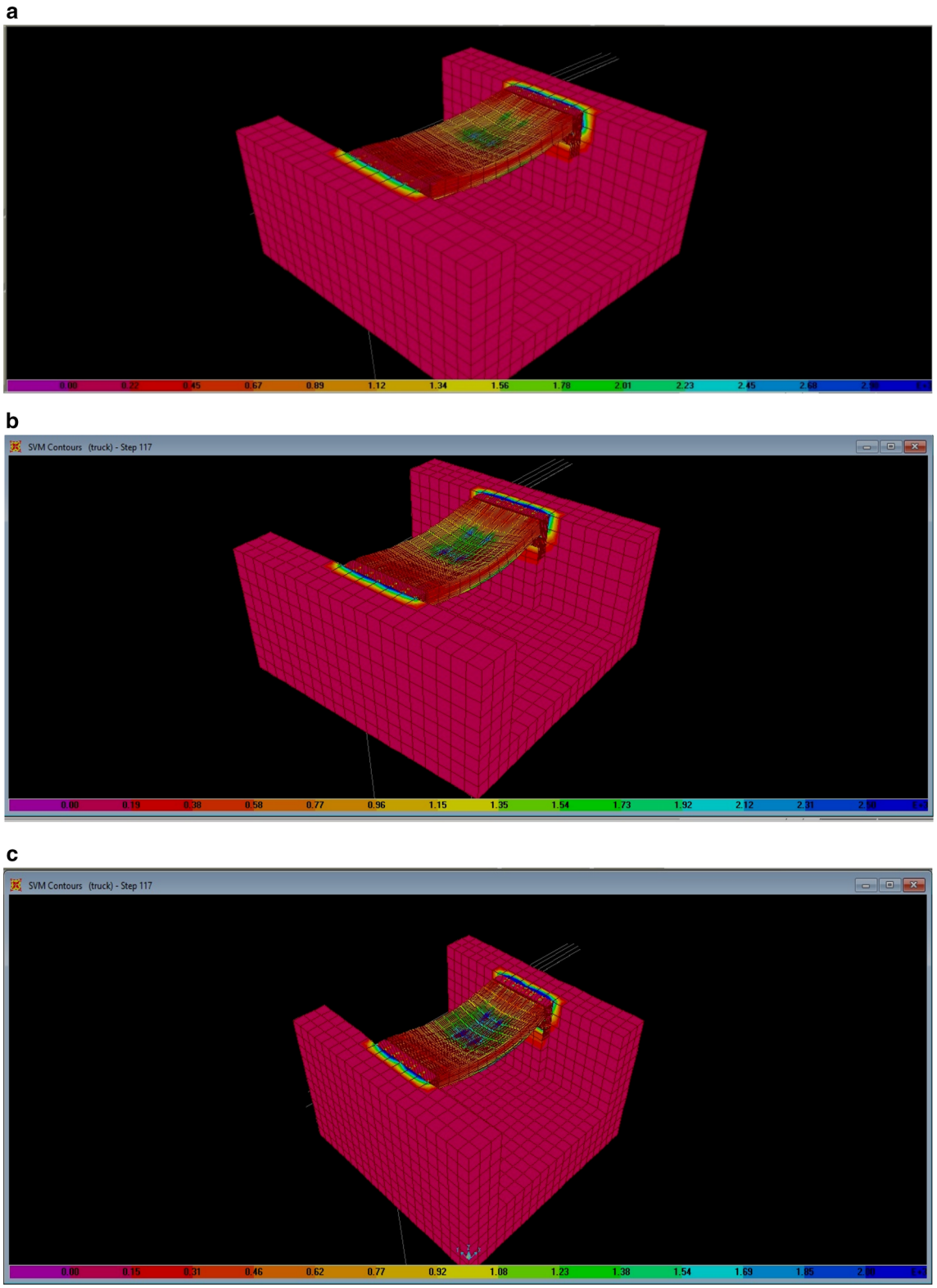

Fig. 17 von Mises stress contours: **a** hard soil, resonant train speed v = 101 m/s; **b** medium soil, resonant train speed v = 95 m/s; and **c** soft soil, resonant train speed v = 73.4 m/s

the structural modifications to be carried out for a continuous connectivity between the abutment and soil.

5 Discussion and Conclusions

This paper attempts to present (1) the utility of SAP2000 FE program to perform dynamic analysis of moving loads and (2) a 3D numerical model to study the effects of vibrations on a small-span simply supported railway bridge. This numerical model was based on direct finite element formulations in the time domain. The high-speed trains were modelled as a set of moving loads, and the results obtained were compared with those discussed by Romero et al. (2013). Following are the conclusions drawn:

- The method followed for performing the dynamic analyses in SAP2000 FE program for the passage of high-speed trains/moving loads can be used to study complex FE problems, pertaining to moving loads.
- The concentrated moving loads analysis is adequate to study the vertical dynamic SSI response of simply supported resonant bridges, since this analysis yielded results that are in fair agreement with the results of the dynamic SSI response of a simply supported resonant bridge subjected to the movement of a multi-body model of HST.
- The resonance frequencies dominate the resonance condition in railway bridges. Resonant train speeds and amplification in the resonant regime were lower when soil–bridge interaction was considered.
- The fundamental periods and damping ratios of the short-span simply supported railway bridge's response were higher when soil–structure interaction was considered than when it was not. It may be affirmed that soil–structure interaction leads to changes in dynamic behaviour.
- The effects of dynamic soil–structure interaction on railway bridges show variations in amplitudes of bridge deck accelerations. Resonance effects were observed at lower operating speeds. Thus, the effects of dynamic soil–structure interaction are an important issue in bridge structure analysis and design.
- Stresses developed at the interface shall warrant the precautions and structural modifications to be carried out for a continuous connectivity between the abutment and soil.

References

Biondi B, Muscolino G, Sofi A (2005) A substructure approach for the dynamic analysis of train-track-bridge system. Comput Struct 83(28–30):2271–2281

Cheng YS, Au FTK, Cheung YK (2001) Vibration of railway bridges under a moving train by using bridge-track-vehicle element. Eng Struct 23(12):1597–1606

Chopra AK (2008) Dynamics of structures theory and applications to earthquake engineering, 3rd edn. Prentice Hall of India, New Delhi

Cook RD, Malkus DS, Plesha ME, Witt RJ (2004) Concepts and applications of finite element analysis, 4th edn. Willey, Hoboken

Delgado RM, Cruz S (1997) Modelling of railway bridge–vehicle interaction on high-speed tracks. Comput Struct 63(3):511–523

Doménech A, Museros P (2011) Influence of the vehicle model on the response of high-speed railway bridges at resonance. Analysis of the additional damping method prescribed by Eurocode 1. In: Proceedings of the 8th international conference on structural dynamics, EURODYN 2011, pp 1273–1280

European Committee for Standardisation (CEN) (2008) Eurocode1: actions on structures—part 2: traffic loads on bridges

Frýba L (2001) A rough assessment of railway bridges for high-speed trains. Eng Struct 23(5):548–556

Hanazato T, Ugai K, Mori M, Sakaguchi R (1991) Three-dimensional analysis of traffic-induced ground vibrations. J Geotech Eng ASCE 117(8):1133–1151

Henriques J (2007) Dynamic behaviour and vibration control of high-speed railway bridges through tuned mass dampers. Dissertation report for the degree of Master of Science in Civil Engineering

Ju SH, Lin HT (2003) Resonance characteristics of high-speed trains passing simply supported bridges. J Sound Vib 267(5):1127–1141

Kausel E, Roesset M (1977) Semianalytic hyperelement for layered strata. J Eng Mech ASCE 103(4):569–588

Kausel E, Roesset M, Waas G (1975) Dynamic analysis of footings of layered media. J Eng Mech ASCE 101(5):679–693

Liu K, Roeck GD, Lombaert G (2009) The effect of dynamic train–bridge interaction on the bridge response during a train passage. J Sound Vib 325(1–2):240–251

Lysmer J, Waas G (1972) Shear waves in plane infinite structures. J Eng Mech ASCE 98(1):85–105

Martınez-Rodrigo MD, Museros P (2011) Optimal design of passive viscous dampers for controlling the resonant response of orthotropic plates under high-speed moving loads. J Sound Vib 330(7):1328–1351

Museros P, Alarcón E (2005) Influence of the second bending mode on the response of high-speed bridges at resonance. J Struct Eng 131(3):405–415

Museros P, Martınez-Rodrigo MD (2007) Vibration control of simply supported beams under moving loads using fluid viscous dampers. J Sound Vib 300(1–2):292–315

Pesterev AV, Bergman LA, Tan CA, Tsao TC, Yang B (2003) On asymptotics of the solution of the moving oscillator problem. J Sound Vib 260(3):519–536

Pyl L, Degrande G, Clouteau D (2004a) Validation of a source–receiver model for road traffic induced vibrations in buildings. II: receiver model. J Eng Mech ASCE 130(12):1394–1406

Pyl L, Degrande G, Lombaert G, Haegeman W (2004b) Validation of a source–receiver model for road traffic induced vibrations in buildings. I: source model. J Eng Mech ASCE 130(12):1377–1393

Rajasankar J, Nagesh RI, Yerraya Swamy B, Gopalakrishnan N, Chellapandi P (2007) SSI analysis of a massive concrete structure based on a novel convolution/deconvolution technique. Sadhana 32(3):215–234

Romero A, Solís M, Domínguez J, Galvín P (2013) Soil–structure interaction in resonant railway bridges. Soil Dyn Earthq Eng 47:108–116

SAP2000 v14.2.4. (2014) Integrated software for structural analysis and Design. User's manual. http://www.csiberkeley.com/products_SAP.html. Accessed 10 Jan 2016

Song C, Wolf JP (1996) Consistent infinitesimal finite-element cell method: three dimensional vector wave equation. Int J Numer Methods Eng 39:2189–2208

Song MK, Noh HC, Choi CK (2003) A new three-dimensional finite element analysis model of high-speed train–bridge interactions. Eng Struct 25(13):1611–1626

Teng YF, Teng NG, Kou XJ (2008) Vibration analysis of continuous maglev guideway considering the magnetic levitation system. J Shanghai Jiaotong Univ (Sci) 13(2):211–215

Ülker-Kaustell M, Karoumia R, Pacoste C (2010) Simplified analysis of the dynamic soil–structure interaction of a portal frame railway bridge. Eng Struct 32:3692–3698

von Estorff O (1991) Dynamic response of elastic blocks by time domain bem and fem. Comput Struct 38(3):289–300

Wang Y, Wei QC, Shi J, Long X (2010) Resonance characteristics of two-span continuous beam under moving high-speed trains. Lat Am J Solids Struct 7:185–199

Wolf JP (1985) Dynamic soil–structure interaction. Prentice-Hall Inc, New Jersey

Wolf JP (1986) A comparison of time domain transmitting boundaries. Earthq Eng Struct Dyn 14:655–673

Wolf JP (1988) Soil–structure-interaction analysis in time domain. Prentice Hall, New Jersey

Wu YS, Yang YB, Yau JD (2001) Three-dimensional analysis of train–rail–bridge interaction problems. Veh Syst Dyn 36:1–35

Xia H, De Roeck G, Zhang N, Maeck J (2003) Experimental analysis of a high-speed railway bridge under Thalys trains. J Sound Vib 268(1):103–113

Xia H, Zhang N, Gao R (2005) Experimental analysis of railway bridge under high-speed trains. J Sound Vib 282(1–2):517–528

Xia H, Zhang N, Guo WW (2006) Analysis of resonance mechanism and conditions of train bridge system. J Sound Vib 297(3–5):810–822

Yang YB, Yau JD (1997) Vehicle–bridge interaction element for dynamic analysis. ASCE J Struct Eng 123(11):1512–1518

Yang YB, Yau JD, Hsu LC (1997) Vibration of simple beams due to trains moving at high-speeds. Eng Struct 19(11):936–944

Yang YB, Chang CH, Yau JD (1999) An element for analysing vehicle-bridge systems considering vehicle's pitching effect. Int J Numer Methods Eng 46(7):1031–1047

Yang YB, Yau JD, Wu YS (2004) Vehicle–bridge interaction dynamics with applications to high-speed railways. World Scientific, Singapore

Yau JD, Yang YB, Kuo SR (1999) Impact response of high-speed rail bridges and riding comfort of rail cars. Eng Struct 21(9):836–844